The Effect of Changing Topological Constraints on Poleward Ocean Heat Transport Induced by Plate Tectonics over the Last 600 Million Years

by

Lorraine Lisiecki

Submitted to the Department of Earth, Atmospheric, and Planetary Sciences
in partial fulfillment of the requirements for the degree of

Master of Science in Geosystems

at the

MASSACHUSETTS INSTITUTE OF TECHNOLOGY

June 2000

Author .....
Department of Earth, Atmospheric, and Planetary Sciences
May 12, 2000

Certified by .....
John Marshall
Professor
Thesis Supervisor

Accepted by .....
Ronald Prinn
Head, Department of Earth, Atmosphere, and Planetary Science

The Effect of Changing Topological Constraints on Poleward Ocean Heat Transport Induced by Plate Tectonics over the Last 600 Million Years

by

Lorraine Lisiecki

Submitted to the Department of Earth, Atmospheric, and Planetary Sciences
on May 12, 2000, in partial fulfillment of the
requirements for the degree of
Master of Science in Geosystems

Abstract

The changing configurations of continents due to plate tectonics is thought to be responsible for some of the variation in climate over the last 600 Ma. Different topological constraints on the oceans may affect their ability to transport heat poleward and change the equilibrium pole-equator temperature of Earth. An ocean model was run for three simple continental geometries to determine the effect of land distribution on the heat transport capacity and pole-equator temperature gradient of the ocean. The first configuration, a circle of land centered over the south pole, meant to resemble Earth at 600 Ma, produces a haline mode of convection in which water sinks in the subtropics. The ocean in this mode has a high pole-equator temperature gradient and low levels of heat transport. The second configuration, a strip of land extending between the north and south poles, resembles the land of the Permian 250 Ma. This configuration with the same atmospheric forcing produces a thermal mode of circulation, similar to the modern North Atlantic, in which surface water sinks at the poles. The ocean in this mode has a lower pole-equator temperature gradient and higher levels of poleward ocean heat transport. A third configuration, similar to the second but with an equatorial ocean passageway, resembles the mid-Cretaceous. This configuration also produces a thermal mode and has slightly higher levels of heat transport than the second model. This research suggests that continental geometry could have played an important role in determining the pole-equator temperature gradient and the levels of ocean heat transport in the past.

Thesis Supervisor: John Marshall
Title: Professor

Acknowledgments

I would like to thank John Marshall and Rhong Zhang for the patience and guidance they provided me as I learned a new subject and carried out this research. I would also like to thank all of the Geosystems professors and students who made this year great. I offer special thanks to my husband Phil and my puppy Stefan who's love and understanding were of great comfort to me during some busy times.

Contents

List of Figures

Chapter 1

Introduction

Earth's climate exhibits large fluctuations; over the last 600 million years, the average global temperature has been as much as 6°C warmer than today [5], and 100 million years ago intermediate-deep ocean temperatures are thought to have been 15°C warmer than at present [4]. The three main factors which lead to climate variability are solar insolation due to Milankovitch cycles, greenhouse warming from varying levels of CO_2 in the atmosphere, and the geometric configuration of landmasses. Continental configuration is important in governing ocean circulation patterns, and thus the amount of heat transported by the ocean. The relationship between continent configuration and ocean heat transport is one of the least understood factors affecting climate. This research will attempt to increase our understanding of the effect of land geometry on the ocean's capacity to transport heat.

Ocean heat transport is one mechanism which mitigates Earth's pole-equator temperature gradient. Differential heating and cooling of the Earth's surface provides more heat to the equator than the poles. Today Earth must transport 6×10^{15} Joules of heat poleward each second to maintain thermal equilibrium [11] . Approximately half of this heat is carried by the ocean as shown in figure 1-1. Changes in the ocean's capacity to transport heat, such as might be caused by plate tectonics, may alter the equilibrium pole-equator temperature gradient and regional climate. In fact, increased ocean heat transport frequently has been proposed as a mechanism by which elevated polar temperatures were maintained during many time periods including the

Late Cretaceous, the Early Eocene, and the Pliocene [11].

Climate reconstructions based on the geologic record of the last 600 million years provide an opportunity to study the mechanisms which contribute to the modern climate and which drive climate change. By studying these mechanisms and their complicated interactions, we increase our ability to predict how the climate may change in the future. Because all the factors which affect climate vary simultaneously, it can be difficult to gain understanding solely from the climate record. The climatic effects of variation in a single factor are most easily studied from climate models where competing effects can be examined in isolation.

The goal of this research is to develop insights about the relationship between the topological constraints imposed on the ocean and its capacity to transport heat. An idealized fluid model of the ocean on a rotating Earth with simple continental shapes will be used to model ocean circulation patterns and pole-equator temperature gradients. Continent configurations which resemble those of the Late Proterozoic 600 Ma (figure 1-2), the Permian 250 Ma (figure 1-3), and the mid-Cretaceous 100 Ma (figure 1-4) are studied. The continents in these models are simple geometric abstractions because the focus of this research is the effect of basic continent location and topological constraints on the ocean. Many details of ocean circulation may be sensitive to the details of coastal geometry, but the ocean's capacity to transport heat, as characterized by the pole-equator temperature gradient, should primarily be a function of gross topology.

For example, one of the simple topologies resembles the Late Proterozoic when all of the land was in the southern hemisphere as shown in figure 1-2. One would expect this land distribution to produce ocean circulation patterns and ocean heat transport levels significantly different from those of today. In fact, decreased poleward heat transport is strongly suggested by the widespread glaciation of the southern hemisphere at that time [5]. The particular shapes of the former coastlines may have influenced the location of certain currents, but the geometry of these coastlines probably did not have a large effect on the level of heat transported poleward by the ocean.

In the next section I provide more details on the mechanisms of ocean heat transport and previous research on the effects of land configuration on the ocean's capacity to transport heat. Then I describe my procedure for configuring the ocean model and for analyzing its results. Finally, I present my results and discuss their significance.

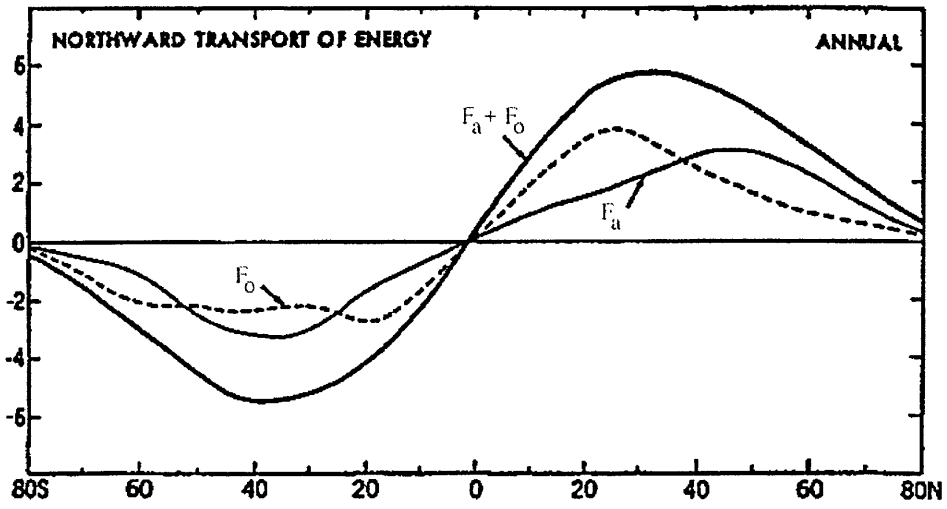

Figure 1-1: **Northward heat transport by the ocean and atmosphere in the present climate**. The flux of heat carried by the ocean F_o is comparable in magnitude to the flux through the atmosphere F_a, from Carissimo et al, 1985 [3].

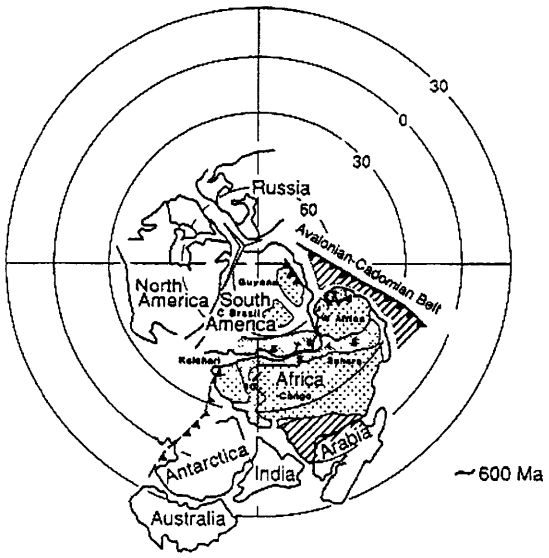

Figure 1-2: **Late Proterozoic land distribution.** The Late Proterozoic supercontinent viewed from the south pole at about 600 Ma from Windley, 1995 [14].

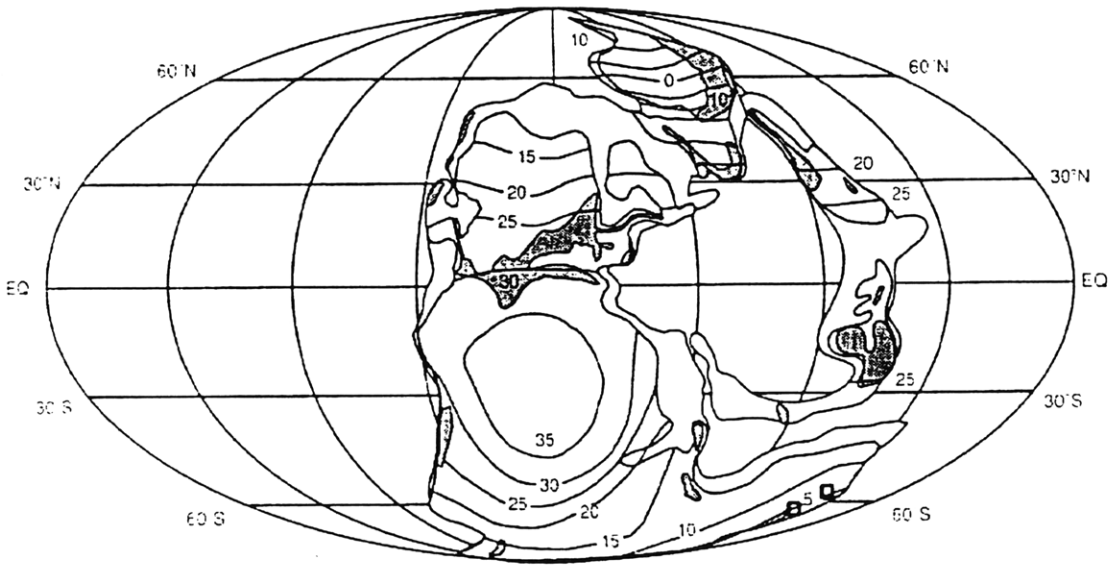

Figure 1-3: **Permian land distribution**. The supercontinent of Pangaea 255 Ma from Crowley and North, 1996 [4]. The contours show modeled January temperatures, and the shading reflects topography.

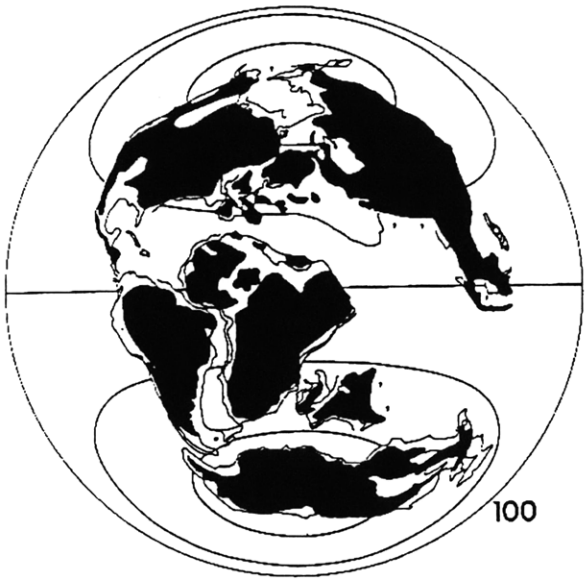

Figure 1-4: **Mid-Cretaceous land distribution**. Land distribution of the mid-Cretaceous 100 Ma from Crowley and North, 1996 [4]. The contours represent 30 and 60 degrees in each hemisphere.

Chapter 2

Background Information

Little research has been done on the relationship between gross topology and ocean circulation. Most studies of the effects of land distribution on ocean heat transport have focused on specific changes, such as the opening and closing of ocean gateways, like the Isthmus of Panama or the Drake Passage, or the coastal geometries of particular paleogeographic reconstructions (e.g., Maier-Reimer et al., 1990 [6]; Mikolajewicz et al., 1993 [8]; Barron et al., 1993 [2]; Sloan et al., 1995 [11]). I will begin this section with some information about the mechanisms of ocean heat transport and the factors which affect it. Then, I will provide some previous research on the effects of continent configuration on ocean circulation and attempt to relate it to how topological constraints might affect the capacity of the ocean to transport heat. Finally, I will discuss research on the extent to which ocean heat transport has varied over the last 600 million years and its effect on global climate.

2.1 Mechanisms of ocean heat transport

The modern ocean transports heat by two main mechanisms: wind-driven circulation and thermohaline circulation [11]. Localized wind-driven circulation is strictly a function of wind velocity and direction, so it may not always transport heat poleward. This circulation is typically swift but confined to the top kilometer of the ocean. Its heat transport capacity is limited by a comparatively small horizontal temperature

gradient as shown in figure 2-1. The thermohaline circulation, is more sluggish but takes advantage of a vertical temperature gradient of about 20°C in the present climate as illustrated in figure 2-1. In only a few polar regions on Earth, surface water becomes more dense than the water below it. This extremely cold water sinks and runs along the ocean floor, rising in warmer regions hundreds of years later [13]. In the Atlantic today, thermohaline convection accounts for 80% of ocean heat transport. However, wind-driven gyres dominate heat transport in the Pacific, where polar waters do not become saline enough to sink. The relative importance of thermohaline versus wind-driven circulation is thought to have varied over geologic time and may be sensitive to the hydrological cycle [15]. Ocean models driven by strong hydrological cycles can support haline modes of circulation in which water sinks in the subtropics instead of at the poles [15]. Figure 2-2 shows the stream function of a haline mode from an ocean model of the Permian [15]. If this mode occurred in the past, the sinking of the warm, salty water in the subtropics probably reduced the amount of heat transported by ocean overturning.

2.2 Role of ocean circulation

Many factors affect the ocean's capacity for heat transport [2]. The atmosphere affects wind-driven circulation directly. It also affects thermohaline convection through changes in air-sea heat flux and fresh water flux. Land configuration plays an important role in controlling atmospheric patterns and places physical constraints on ocean circulation, both of which affect the heat transport mechanisms of the ocean. The surface buoyancy flux of the ocean B determines where and how much surface water sinks and is given by

$$B = \frac{g}{\rho_o}\left(\frac{\alpha_\vartheta}{c_w}\mathcal{H} + \rho_o \beta_S S(E-P)\right) \tag{2.1}$$

where g is gravitational acceleration, ρ_o is the constant reference density 1000 kg m^{-3}, α_ϑ and β_S are the thermal expansion and haline contraction coefficients, c_w is the heat capacity of water, $\mathcal{H}$ is the surface heat loss, and $E-P$ is evaporation minus

precipitation in units of velocity.

One idea relating ocean heat transport to land configuration suggests that if an ocean basin is confined to a particular latitude or allowed to circle the globe unhindered at a certain latitude, it will achieve a temperature in equilibrium with the air temperature of that latitude [12]. An example of this phenomenon is the modern Antarctic Circumpolar current which has some of the coldest surface water on the planet [12]. Another example is the Cretaceous Neotethyan Seaway that existed 80 million years ago [12]. This seaway may have allowed the ocean to flow almost unimpeded completely around Earth at near equatorial latitudes. There is some evidence that this water attained temperatures well in excess of those of modern-day tropical oceans [12]. This concentration of heat at the equator would have produced a high pole-equator temperature gradient. Oceans which remain at a relatively constant latitude may exchange less heat with water at other latitudes and reduce poleward heat transport. Other evidence shows that mid-Cretaceous equatorial temperatures may have been similar to those of the present day [4] (figure 2-3), so the mid-Cretaceous may actually have had a relatively small pole-equator temperature gradient. This is discussed further in the section on paleoclimate reconstructions.

The importance of ocean gateways on ocean heat transport has been the subject of several studies. These passages connect one ocean to another and are important because they prevent the connected ocean basins from varying too widely in temperature or salinity. Their openings and closings can cause major changes in global ocean circulation patterns and change the efficiency of poleward heat transport. For example, thirty million years ago the Drake Passage between South America and Antarctica opened [8] and permitted water to circulate unimpeded around the south pole, leading to the thermal isolation of Antarctica. The cooling effect of this isolation is suggested by the close correspondence in time between the opening of Drake Passage and the commencement of glaciation on Antarctica [8]. The research on ocean gateways suggests that not only continent location but also ocean connectedness is very important in determining the heat transport capacity of the oceans. Due to the very simple configurations of the continents in the model runs, this issue is only

explored to a very limited extent in this study.

Detailed bathymetry can also influence flow patterns. Poulsen et al. [10] studied surface circulation of the mid-Cretaceous Tethys. They found that small changes in the width or depth of the sill, the latitude of the strait, or the southern extent of southeast Asia produced significant changes in the circulation of Tethys. However, their results do not indicate what effect these changes had on ocean heat transport. The significance of detailed features on the pole-equator temperature gradient should be assessed in future research.

In addition to uncertainties about which factors affect ocean heat transport and to what extent, uncertainty exists about the importance of ocean heat transport in altering global climate over the last 600 million years. A study by Barron et al. [2] found that small increases in ocean heat transport in the Cretaceous resulted in tropical ocean surface temperature changes, polar warming, and weakened temperature gradients. They concluded that changes in ocean heat transport could produce significant climate changes including increases in the globally averaged surface temperature. However, the climate changes they observed were unable to fully reproduce the conditions in the Cretaceous suggested by the paleorecord. They concluded that the effects of altered ocean heat transport alone were not sufficient to explain Cretaceous warmth. They also found that increasing the level of heat transport did not change the structure of the general circulation of the ocean or atmosphere outside of the tropics and deduced that the land-sea distribution of the Cretaceous was responsible for the modeled circulation pattern.

Sloan et al. [12] calculated from paleotemperature data that the level of poleward heat transport for the Early Eocene may have been 30% higher than for the present. After examining the proposed methods of increased oceanic heat transport for that period, they concluded that these mechanisms were probably accompanied by feedback mechanisms or increased atmospheric heat transport to achieve the climatic conditions of the Early Eocene. In particular, they suggest that the effects of increased poleward oceanic heat transport are limited to warming high-latitude oceans and coastal regions and cooling low latitudes slightly.

My research focuses on the poorly understood role of land-sea distribution and general topological constraints on ocean heat transport rather than the effects of small gateways or detailed topography. It provides evidence that ocean topology alone is sufficient to produce significant effects on ocean circulation, and what those effects are. Because of the particular configurations examined, this research can also help to estimate the level to which ocean heat transport may have varied over the last 600 million years. However, because the atmosphere is not fully coupled to the ocean in the model we use, inferences about the climatic effects of changes in heat transport must be made with care.

According to the presented theories, the model run with the band of land extending from north to south should have the highest rate of poleward heat transport and the lowest pole-equator temperature gradient. Because ocean currents cannot circle Earth, this land distribution should increase the latitudinal movement of the ocean waters which will increase the amount of heat transported poleward. The model with all of the land centered over the south pole should exhibit the highest pole-equator temperature gradient. The range of temperature gradients observed is probably a strong function of the atmospheric forcing which in our calculations are kept fixed. Nevertheless, the results may provide a guide to possible variations. There may be a correlation between the pole-equator temperature gradients of the simple models and the paleorecord. These results would support the hypothesis that land distribution has a strong influence on global climate.

2.3 Paleoclimates of 600 Ma, 250 Ma, and 100 Ma

The climate of the late Precambrian 600 Ma is not well observed or understood. This point in time marks the end of a 300 million year period of glaciation and the end of a supercontinent (figure 1-2). Geologic evidence shows that glaciation was widespread, extending into the low latitudes [4]. The extensive cold of this time may be the result of a solar luminosity output 5-10% lower than modern levels [4]. Very little theoretical work has been done to understand the climate of this period.

Another period of glaciation ended in the Early Permian [4]. The supercontinent of Pangaea came together during the mid-Permian 250 Ma (figure 1-3)[4]. The climate of this continent was generally dry and seasonal with warm temperatures at the equator and cold temperatures at the poles [4]. Modeling shows that a strong western boundary current in Panthalassa carried heat poleward [4]. The paleorecord does show warmer temperatures on the eastern coast of Pangaea, and because the current was downwind of the continent, the current may not have had a large effect farther inland [4].

The mid-Cretaceous 100 Ma (figure 1-4) has been studied more extensively. Species extents and $\delta^{18}O$ records indicate that high and mid latitudes may have been much warmer than today [4]. Low latitudes have long been assumed to have also been warmer than present, but recent evidence shows that tropical temperatures may have been similar to those of the present [4]. Figure 2-3 shows the range of estimated mid-Cretaceous temperatures. Elevated CO_2 levels, previously cited as a probable cause of warming, would have raised equatorial temperatures 4-5°C [4]. If low latitude temperatures were near present levels, then some other mechanism, such as high levels of ocean heat transport, would be needed to explain the high-latitude warmth. GCM's suggest that elevated ocean heat transport may not produce high enough polar temperatures [4], but these temperatures are still not known with a great degree of accuracy [4].

If a simple theory can be formulated to relate landmass distribution and topological constraints on the ocean to the pole-equator temperature gradient, it could help paleoceanographers determine the effects of other paleogeographic and climate factors on ocean heat transport. Improving our understanding of ocean heat transport also increases our understanding of climate variability as a whole. These results will improve our ability to use knowledge of the paleorecord to gain information about the current and future climate of Earth.

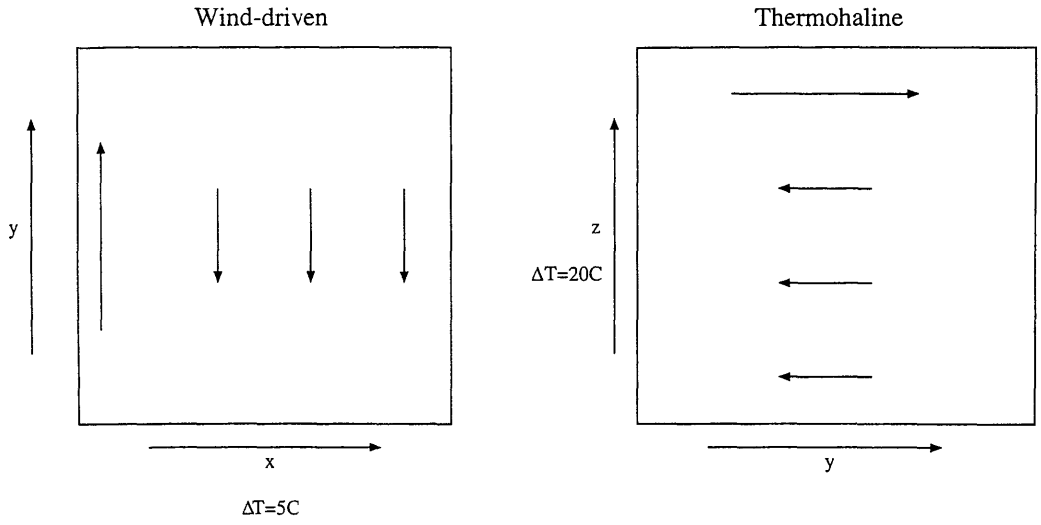

Figure 2-1: **Wind-driven versus thermohaline circulation.** Wind-driven circulation transports heat by the zonal movement of water which has a temperature difference of only about 5°C. Thermohaline circulation transports heat by the movement of water meridionally. The water moving toward the pole at the surface is about 20°C warmer than the water at depth.

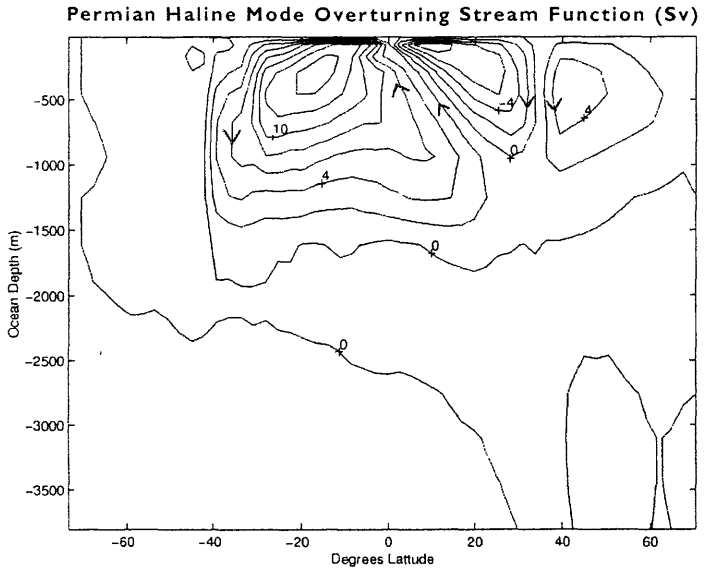

Figure 2-2: **Haline circulation produced in a model of the Permian.** This haline circulation was produced by a model of the Permian [15] with strong hydrological forcing.

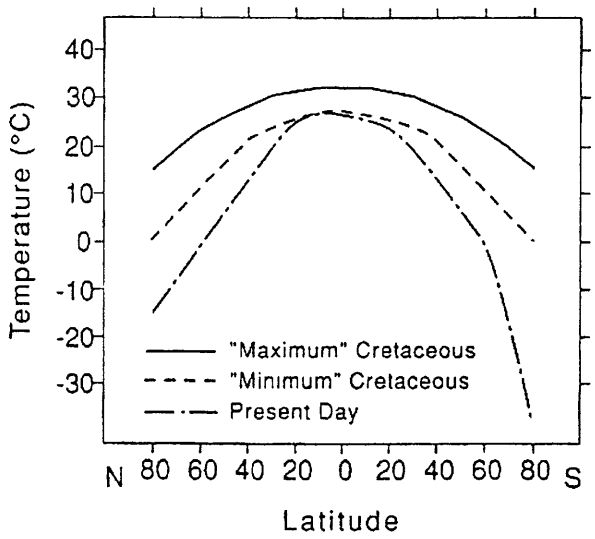

Figure 2-3: **Range of uncertainty in Cretaceous temperatures.** If low latitude temperatures were similar to those of the present day, then the pole-equator temperature gradient would have been very small, perhaps as the result of increased ocean heat transport, and it is less likely that polar warmth was the result of increased levels of CO_2. (from Barron et al. [1])

Chapter 3

Experimental Method

A series of experiments was carried out using an ocean general circulation model (GCM) to try to determine the effect of land-sea distribution on poleward ocean heat transport. The selection of idealized landmass distributions considered is motivated by the paleorecord. In examining the results, I focus my attention on the steady-state mode of circulation and the pole-equator temperature gradient relative to the prescribed atmospheric temperature.

3.1 Ocean GCM

The ocean model developed by Marshall et al. [7] integrates forward in time the equations that govern the evolution of a fluid on a rotating sphere. The state of the ocean is characterized by the distribution of currents $\mathbf{v}$, the potential Temperature T, salinity S, pressure p, and density ρ. The evolution of these fields is determined by applying the laws of classical mechanics and thermodynamics to an incompressible fluid and making the hydrostatic approximation. Using the coordinate x for the east direction, y for the north, and z for up in the vertical direction, the resulting equations are

Motion

$$\frac{\partial \mathbf{v_h}}{\partial t} = \mathbf{G_{v_h}} - \nabla_h p \tag{3.1}$$

Continuity

$$\nabla \cdot \mathbf{v} = 0 \tag{3.2}$$

Heat

$$\frac{\partial T}{\partial t} = F_T \tag{3.3}$$

Salt

$$\frac{\partial S}{\partial t} = -\nabla \cdot (\mathbf{v}S) + F_S \tag{3.4}$$

Equation of state

$$\rho = \rho(T, S, p) \tag{3.5}$$

where

$$\mathbf{v} = (\mathbf{v_h}, w) = (u, v, w) \tag{3.6}$$

is the velocity in the zonal, meridional, and vertical directions, respectively, given by

$$p = \frac{\delta p}{\rho_{ref}} \tag{3.7}$$

and where δp is the deviation of the pressure from that of a hydrostatically balanced ocean at rest and

$$\mathbf{G}_v = (G_u, G_v, G_w) \tag{3.8}$$

are inertial Coriolis, metric, gravitational, and forcing/dissipation terms in the zonal, meridional, and vertical direction. F_T and F_S are the forcing functions for heat and salt derived from the air temperatures and net evaporation $(E - P)$ shown in figures 3-3 and 3-4.

$$F_T = -\frac{\partial}{\partial z}\mathcal{H}_T \tag{3.9}$$

where the vertical heat flux $\mathcal{H}_T$ is given by the vertical diffusivity of heat κ_v and the vertical temperature gradient

$$\mathcal{H}_T = \kappa_v \frac{\partial T}{\partial z} \tag{3.10}$$

in the ocean's interior and given by the difference between the sea surface and air temperature $(SST - T_A)$

$$\mathcal{H}_T = -4dc_a u_w \rho_o C_p (SST - T_A) \tag{3.11}$$

at the ocean's surface where u_w is the wind speed, c_a is heat capacity of air equal to 1.004 J/m^3/°C, d is the drag coefficient which has a value of 1.3, and C_p is the specific heat of water at constant pressure. $\mathcal{H}_T$ is zero at the ocean bottom. Similarly,

$$F_S = -\frac{\partial}{\partial z}\mathcal{H}_S \tag{3.12}$$

where the vertical salinity flux $\mathcal{H}_S$ is

$$\mathcal{H}_S = \kappa_v \frac{\partial S}{\partial z} \tag{3.13}$$

and

$$\kappa_v \frac{\partial S}{\partial z} = S(E - P) \tag{3.14}$$

at the surface, and the vertical salinity gradient at the ocean floor is zero.

Unlike the prognostic variables u, v, w, T, and S, the pressure field must be obtained diagnostically. The equations of motion and continuity lead to a three-dimensional elliptic equation for pressure which is inverted using the pressure method [9]. Finite volume techniques are used to discretize the equations as described in Marshall et al. [7].

The ocean has a free surface which is treated implicitly. No normal flow is allowed through the sides or bottom of the ocean basin. Additionally, the diffusive fluxes of heat and salt are set to zero at the ocean bottom and sides. The system is driven by the prescribed, zonally symmetric wind stress, surface air temperatures, and fresh water flux shown in the figures 3-2, 3-3, and 3-4. The wind stress used is designed to simulate Permian conditions and is weaker than the present-day wind stress. The fresh water flux is similar to the present-day flux and is adjusted slightly in each model so that evaporation was equal to precipitation integrated over the ocean's surface. In the model with the large continent over the southern pole, fresh water was added to the ocean surface uniformly along the continental boundary to simulate runoff. In the other two models, the net imbalance of fresh water flux resulting from the placement of the continents was distributed uniformly over the ocean surface.

The ocean GCM was run with a resolution of 4.5 degrees in longitude and latitude and 15 depth levels in all cases. The mixing timescale of the global ocean in this model is a few thousand years. With the selected resolution, the model can be 'spun-up' to steady state in about 64 hours of cpu time on eight processors of an SGI machine. The model is designed to utilize parallel computers and was run on clusters of Suns, SGI's, and Intel machines at MIT and Boston University. The models were run for 4000 model years, after which they had achieved steady state shown in figure 3-5.

The model outputs the complete state of the system, including velocity, pressure, temperature, and salinity. Analysis of the experiments focuses on the steady-state pole-equator temperature gradient and quantity of heat transported in the different model runs. Heat is transported by two mechanisms: mean meridional velocity heat transport Q_v, defined as

$$Q_v = \iint \rho C_p v T \, \mathrm{d}x \, \mathrm{d}z \tag{3.15}$$

where ρ is the ocean density, C_p is the specific heat of water, x is the zonal direction and z is the vertical direction, and eddy heat transport Q_e, defined as

$$Q_e = -\iint \rho C_p \kappa_h \frac{\partial T}{\partial y}\, \mathrm{d}x\, \mathrm{d}z \tag{3.16}$$

where κ_h is horizontal diffusivity and y is the meridional direction. Using the simple topologies, I attempt to correlate pole-equator temperature gradient to landmass distribution in the context of the paleorecord.

3.2 Simple land distributions

Figure 3-1 shows the land-sea distributions which are studied. They were selected to feature simple and distinct topologies, and to resemble geographies derived from plate reconstructions [16]. The percentage of Earth's surface covered by land is held constant at 39% for all of the topologies. The depth of the ocean basins is four kilometers everywhere. All of the configurations also feature a small cap of land over the poles to ease computational problems associated with converging meridians. The first landmass distribution consists of a circle of land centered over the south pole that extends to a latitude of 17.5°S with an ocean extending to 72°N. This configuration resembles the land-sea distribution of the Late Proterozoic, 600 Ma (figure 1-2). The second distribution studied is a 112.5°-wide strip of land extending from the north to south pole with caps of land over each pole extending down to 67.5 degrees. This configuration is meant to resemble the geography of the Permian, 250 Ma ago (figure 1-3). A similar north-south strip of land 148.5° wide with a 18°-wide ocean passageway at the equator and the same polar caps as the previous model represents the land distribution of the mid-Cretaceous (figure 1-4).

a) Land in South

b) North–South Strip

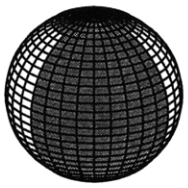

c) Equatorial Passageway

Figure 3-1: **The three simple land configurations used in the model**. a) This configuration designed to resemble the landmass distribution 600 Ma BP consists of a large landmass over the south pole extending to a latitude of 18°S and a small north polar cap extending to 72°N. b) A strip of land 112.5° wide extends from the north pole to the south pole and caps on each pole reach 67.5°. This distribution is meant to resemble the continental configuration at 250 Ma BP. c) This north-south strip of land is 148.5° wide and has an ocean passage way 18° wide centered over the equator. The polar caps again extend to 67.5°. This configuration represents the landmass distribution on Earth 100 Ma BP.

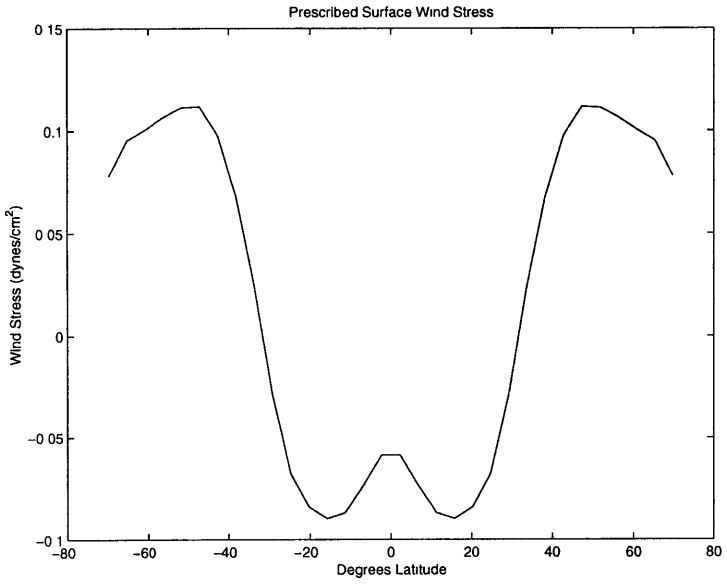

Figure 3-2: **Prescribed wind stress at ocean's surface.** This wind stress based on the wind stress of the Permian is zonally symmetric and is used in all three model runs.

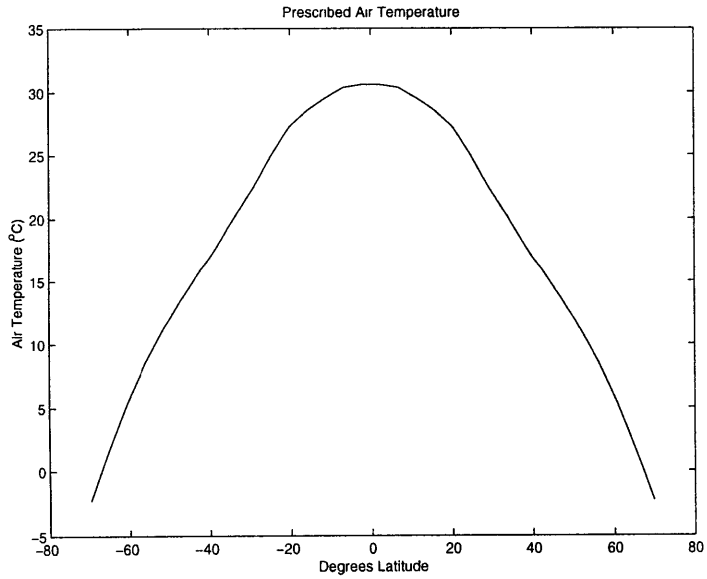

Figure 3-3: **Prescribed surface air temperature.** The prescribed surface air temperature is zonally symmetric and is used to calculate the flux of heat $\mathcal{H}_T$ into and out of the ocean's surface.

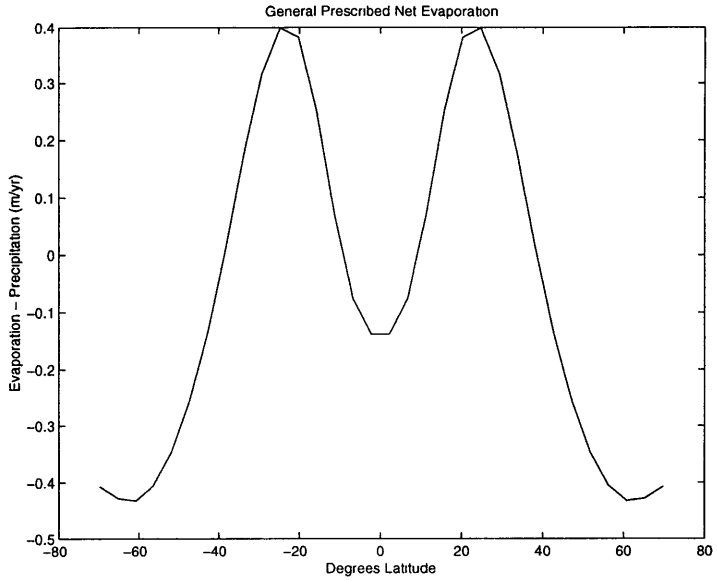

Figure 3-4: **Form of prescribed net evaporation.** The difference between evaporation and precipitation is zonally symmetric and is used to determine the salinity flux $\mathcal{H}_S$ at the ocean's surface. It is not identical for each run because small adjustments are needed so that the net salinity flux integrates to zero over the ocean's surface. These slight changes are reflected in the salinity buoyancy fluxes provided in the results section.

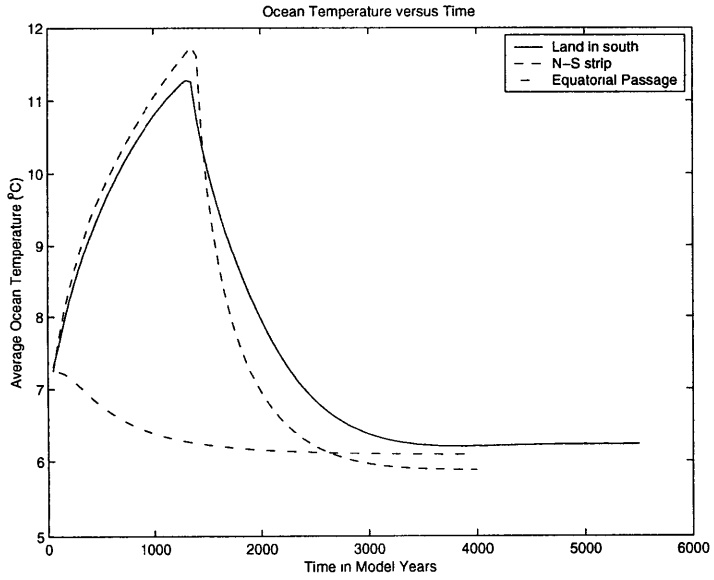

Figure 3-5: **Mean ocean temperature versus time in model years.** After 4000 years of model time, the three-dimensional average temperature of the ocean becomes constant, indicating that all three runs have achieved equilibrium.

Chapter 4

Results

4.1 No meridional barrier

The first land distribution examined, the one with all of the land in the south, allowed ocean currents to flow unimpeded around the Earth at constant latitude. The vertically integrated horizontal stream function in figure 4-1 shows a maximum circulation of about 65 Sv at a latitude of 25°N. The overturning stream function in figure 4-2 shows a large convection cell in which water sinks at about 35°N and rises at the equator, in a pattern indicative of the haline mode of circulation. The overturning circulation has a strength of 10 Sv and reaches all the way to the floor of the ocean. A smaller convective cell of only 3 Sv occurs in the northern subpolar region; in this cell, water sinks at 35°N and rises at 70°N. The reason for this pattern of vertical motion can be seen in figure 4-3 which shows the flux of buoyancy out of the ocean surface. The thermal forcing near the north pole is very weak and is nearly balanced by the haline forcing. Near 25°N the thermal and haline forcing are both positive and enough buoyancy is lost to induce sinking. A plot of heat transport in figure 4-4 reveals that mean meridional velocity heat flux and eddy heat flux are almost equal in magnitude. Heat transport reaches a maximum of 1.1 pW at 20°N. The difference between the sea surface temperature and the air temperature, shown in figure 4-14, is small.

4.2 Meridional barrier

The second land distribution, with the strip of land extending from the south to the north poles, prevented ocean currents from circling the globe. The westward equatorial current is forced to diverge to the north and south when it reaches the land. This forms two symmetric gyres, one in each hemisphere, shown in figure 4-5. The zonally integrated overturning stream function looks very different from the previous run and reveals that the ocean is convecting in a thermal mode similar to the present, in which cold water sinks at the poles and rises near the equator. The stream function has a maximum value of 20 Sv at 60° north and south. With this land distribution the thermal buoyancy flux shown in figure 4-7 is much larger than the haline flux, creating a large and outward flux of buoyancy near the poles. Figure 4-8 shows that the majority of heat is now transported by the mean meridional velocity; the eddy heat transport is much smaller. The poleward heat transport reaches a maximum of 1 pW at 40° north and south. The difference between the sea surface temperature and the air temperature is larger at the equator and poles than it is in the previous case with no meridional barrier.

The third land distribution, the one with the equatorial passage through the north-south strip, has very similar results to the second distribution. The vertically integrated horizontal stream function in figure 4-9 shows one large gyre in each hemisphere and a flow of 10 Sv through the equatorial passage. The zonally integrated overturning stream function in figure 4-10 is nearly identical to the stream function of the north-south strip run, but it is slightly stronger. In figure 4-11 the thermal component of the buoyancy forcing is also larger. The eddy component of heat transport is once again small. The total heat transport shown in figure 4-12 is slightly larger than that of the solid north-south strip between 40°S and 40°N.

4.3 Heat transport capacity

The levels of heat transport for these three runs should not be directly compared because they represents the heat transported by different extents of ocean at each latitude. By looking at figure 4-13, a plot of heat transport per kilometer of ocean at each latitude, one can see that the ocean transports about half as much heat when all of the land is in the south. This effect is also demonstrated by the difference between sea surface temperature and prescribed air temperature for the three model runs in figure 4-14. The zonally averaged, surface pole-equator temperature gradients from the equator to 67.5°N are 26.6°C for the land in the south, 24.5°C for the north-south strip, and 23.9°C for the strip with the equatorial passage. These gradients provide further evidence for the reduced ocean heat transport in the haline mode and its possible effect on Earth's climate.

The three-dimensional average ocean temperature is also different for the three model runs. The run with all of the land in the south has an average temperature of 6.2° C. The north-south strip has an average temperature of 5.9°C, and the strip with the equatorial passage has an average ocean temperature of 6.1°C. The different mean temperatures are probably the result of the different latitudes occupied by the oceans of each model. The oceans' abyssal temperatures are 2.3°C, 4.7°C, and 4.8°C, respectively. The run with the land in the south has a considerably colder abyssal temperature presumably because the ocean extends farther to the north where the prescribed atmospheric temperature is much smaller. The abyssal temperature of the equatorial passage is probably slightly higher because a higher rate of heat transport has produced warmer polar waters.

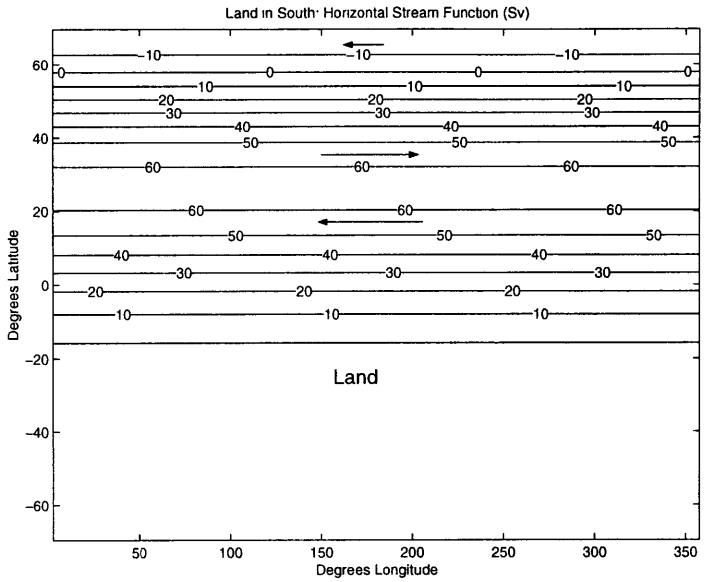

Figure 4-1: **Vertically integrated horizontal stream function for the distribution with all of the land in the south.** Ocean currents flow around Earth at constant latitude with little meridional motion. The ocean in this model is zonally symmetric.

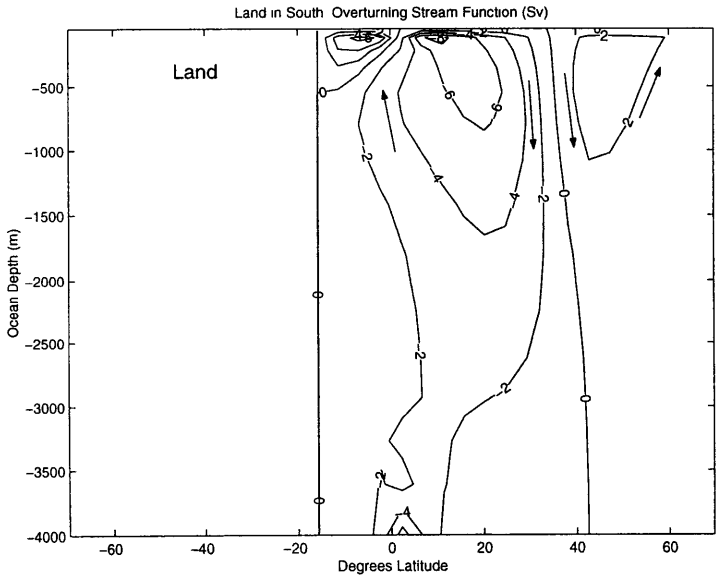

Figure 4-2: **Zonally integrated vertical stream function when the land is in the south.** This overturning circulation is characteristic of a haline mode. Warm, salty water sinks in the subtropics. Because there are no land barriers, the haline circulation reaches all of the way to the ocean floor.

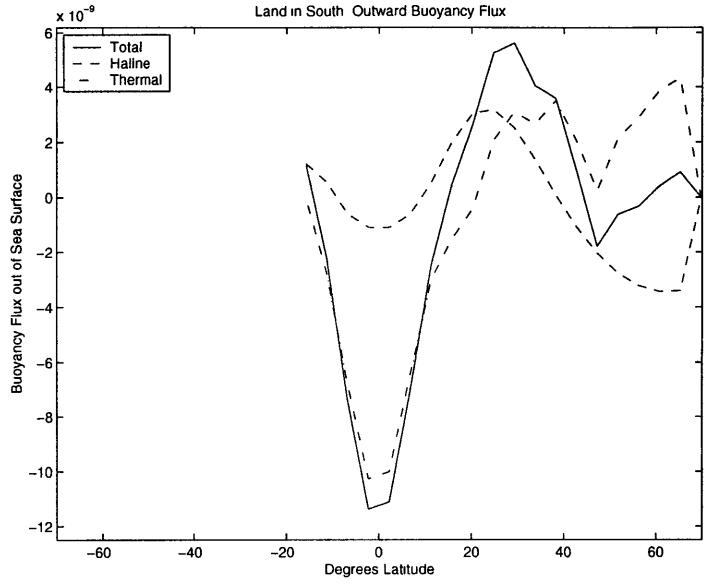

Figure 4-3: **Zonally symmetric surface buoyancy flux out of the ocean's surface when the land is in the south.** The thermal and haline forcing are approximately equal and opposite in the high northern latitudes, but in the subtropics the two add to produce a net outward flux which results in the sinking of warm water in low latitudes.

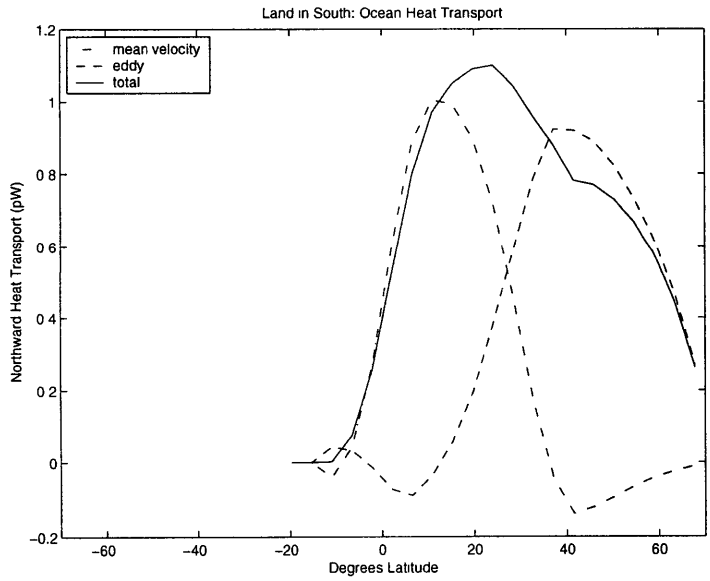

Figure 4-4: **Zonally integrated ocean heat transport when the land is in the south.** The eddy and mean meridional heat transports are of approximately equal size.

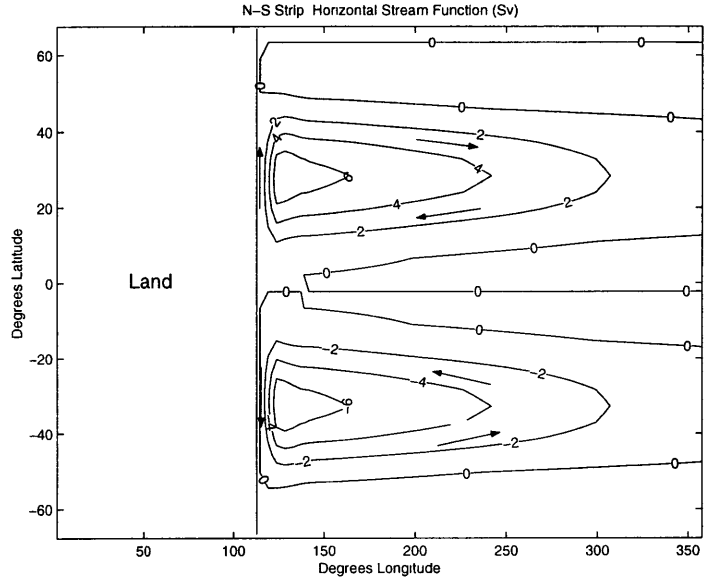

Figure 4-5: **Vertically integrated horizontal stream function when land is in a north-south strip.** The westward equatorial current is diverted toward the poles at the continent's eastern boundary.

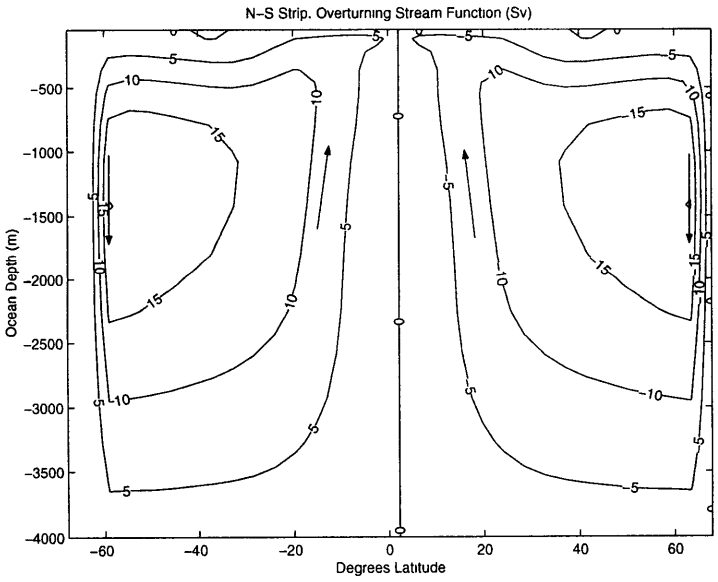

Figure 4-6: **Zonally integrated vertical stream function when the land is in a north-south strip.** Surface water sinks at the poles. This is a good example of the thermal mode of convection.

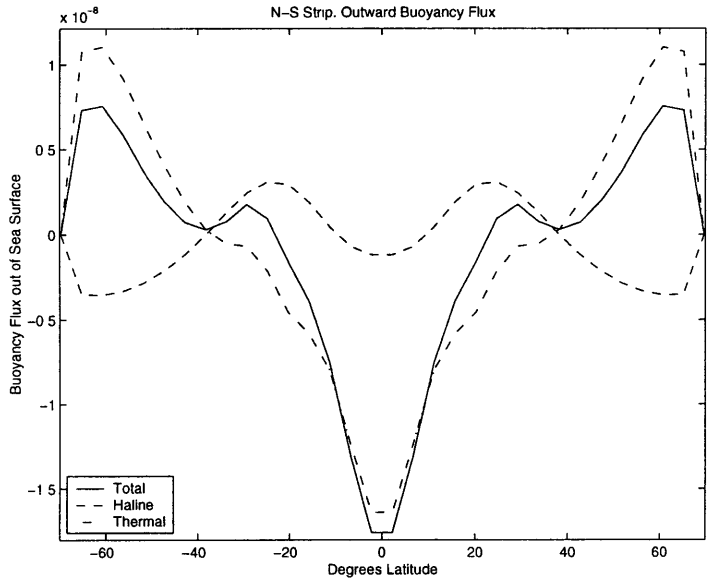

Figure 4-7: **Zonally averaged buoyancy flux out of the ocean when the land is in a north-south strip.** The thermal contribution to the buoyancy flux is very large at the poles, and the total buoyancy flux at the poles is much larger than that in the subtropics, creating a thermal mode of convection.

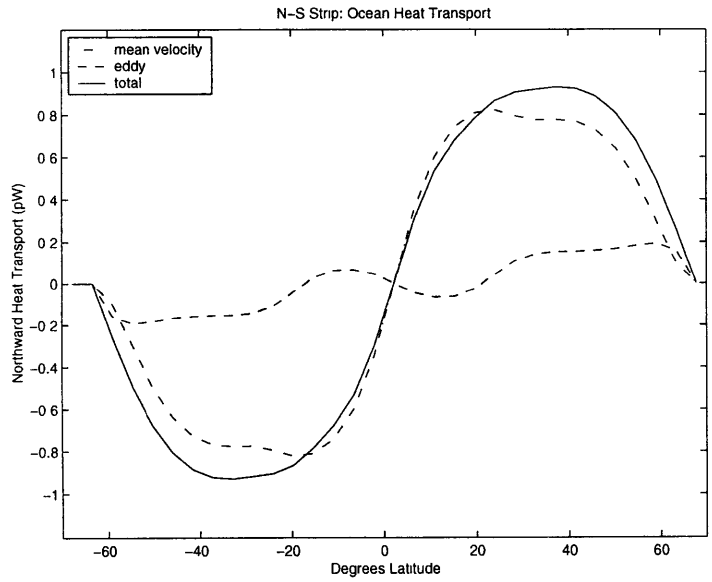

Figure 4-8: **Zonally integrated ocean heat transport when the land is in a north-south strip.** The mean meridional velocity transport is much greater than the eddy transport.

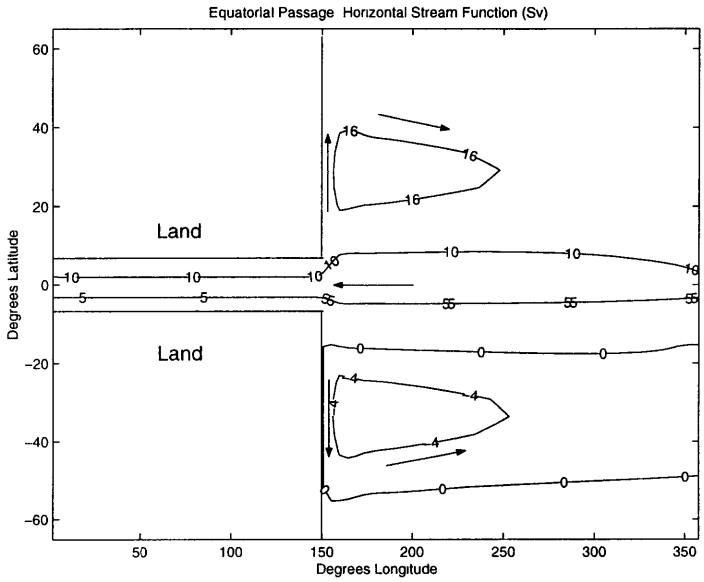

Figure 4-9: **Vertically integrated horizontal stream function when land is in a north-south strip with an equatorial passageway.** The flow through the passage is about 10 Sv.

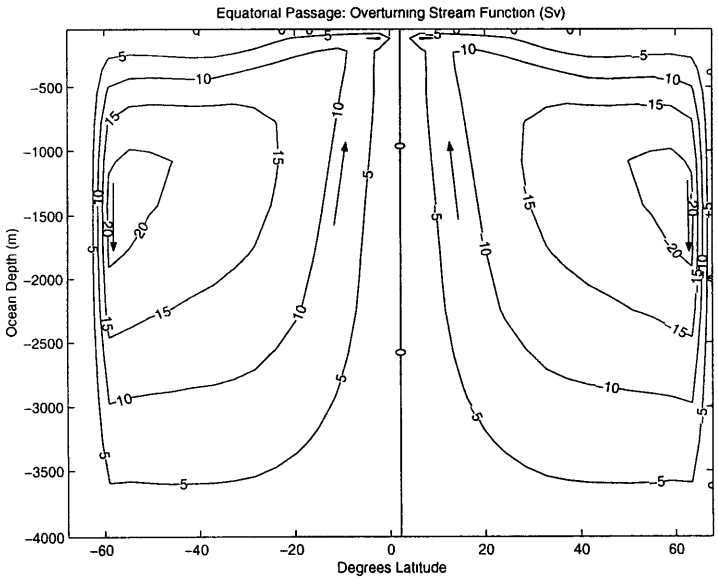

Figure 4-10: **Zonally integrated vertical stream function when land is in a north-south strip with an equatorial passageway.**

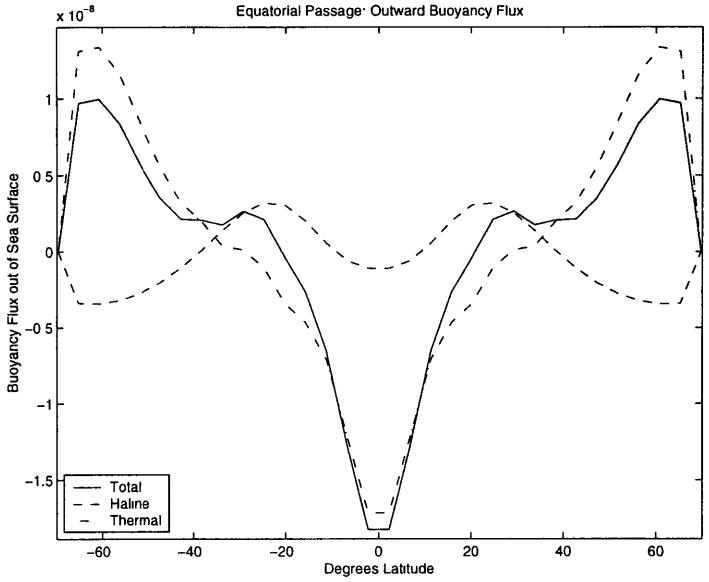

Figure 4-11: **Zonally averaged buoyancy flux out of the ocean when the land is in a north-south strip with an equatorial passageway.** The buoyancy flux is very similar to the strip with no passageway, but the fluxes are slightly higher in magnitude.

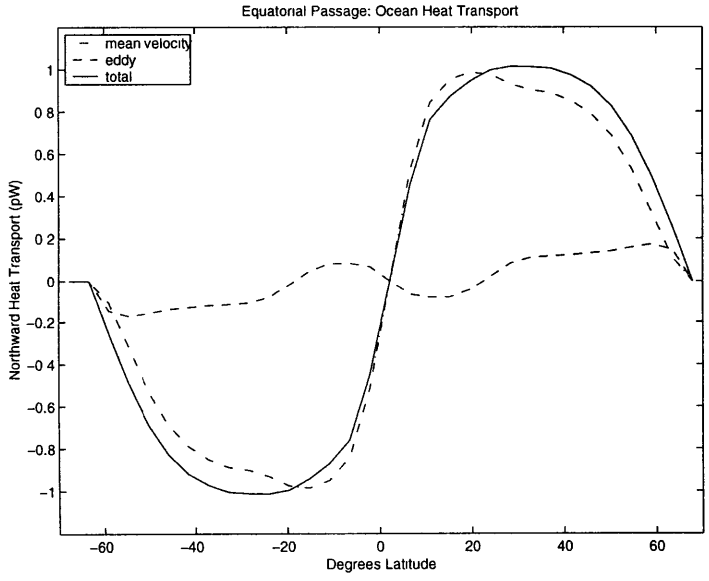

Figure 4-12: **Zonally integrated ocean heat transport when the land is in a north-south strip with an equatorial passageway.** The heat transport is very similar to the case with no equatorial passage but with a slight anomaly in eddy heat transport near the northern edge of the passageway.

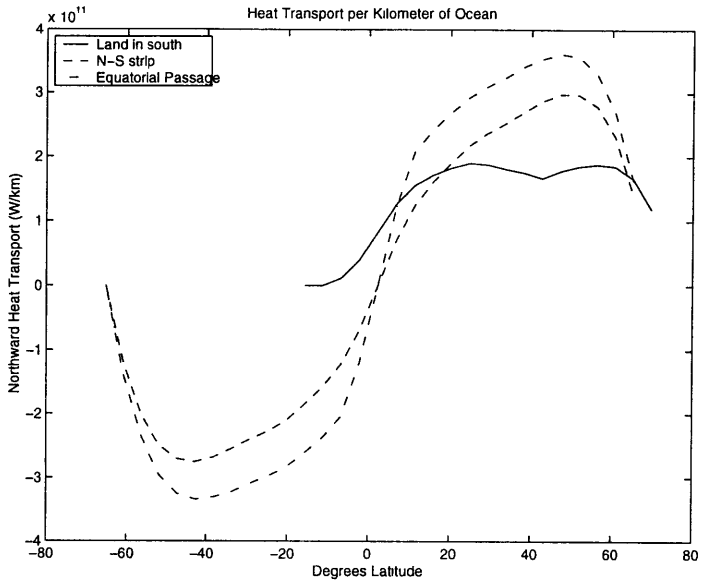

Figure 4-13: **Average ocean heat transport per kilometer of zonal ocean extent.** When normalized for the extent of ocean available to transport heat, it becomes clear that when all of the land is in the south, the ocean transports heat less efficiently. Additionally, the land distribution with an equatorial passageway and a wider strip of land, transports more heat per kilometer of ocean than the case with no equatorial passage.

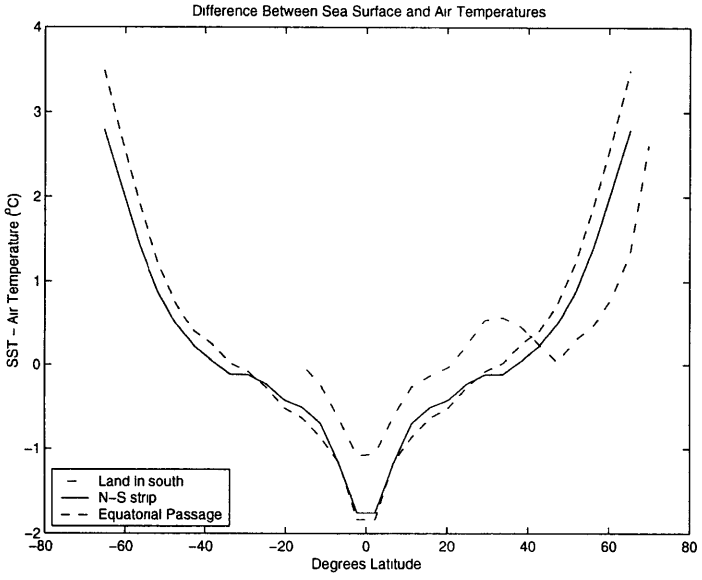

Figure 4-14: **Zonally averaged difference between sea surface temperature and prescribed air temperature.** The run with the land in the south has a much smaller deviation from the prescribed air temperature. It is also warmer in the subtropics than the other two runs. The land distribution with the equatorial passage is warmer at the poles and slightly cooler at the equator than the strip of land with no passage.

Table 4.1: **Ocean heat characteristics of three simple land distributions.**

	Land in south	N-S Strip	Eq. Passage
Maximum heat transport per km of zonal ocean extent (10^{11} W/km)	1.9	3.0	3.6
0-67.5 N temperature gradient (°C)	26.6	24.5	23.9
Abyssal ocean temperature (°C)	2.3	4.7	4.8
3-D average ocean temperature (°C)	6.2	5.9	6.1

Chapter 5

Discussion

The results from the these three model runs demonstrate that changes in the distribution of land on Earth can greatly affect the circulation of the ocean and its heat transport. When all of the land is in the south, the prescribed surface ocean fluxes produce a haline mode of ocean circulation. This haline mode of circulation is stable for at least eight thousand years of model time. A thermal mode of circulation is produced by the same model when only the distribution of land is changed. This demonstrates that the distribution of land on Earth is very important in determining the pattern and mode of ocean circulaton. The thermal mode observed in the last two model runs has a much higher heat transport capacity than the haline mode. Interestingly, the run with the equatorial passageway had a slightly higher heat transport than the run with the solid strip. This may be related to the narrowness of the passageway or the increased thickness of the strip necessary to preserve the ratio of land to ocean area. The sea surface temperature varied by only 3°C between the model runs. A larger temperature difference could probably have been obtained by stronger surface winds, but atmospheric feedbacks would also affect the size of sea surface temperature change.

The model run with the land in the south suggests that the ocean of the Late Proterozoic should have had relatively low levels of heat transport. Evidence from the paleorecord, such as extensive glaciation, suggests that this was a time of low heat transport [5]. These results also support the theory put forth by Stanley that oceans

with no meridional barriers transport less heat [12]. The other two model runs suggest that ocean heat transport was much larger and that the pole-equator temperature gradient was smaller in the Late Permian and Late Cretaceous. The warm east coast of Pangaea supports the theory that this was a time of high ocean heat transport [4]. The results of this simple model support the idea that the mid-Cretaceous was a period with a low pole-equator temperature difference, and does not support the use of the mid-Cretaceous as an example of Stanley's theory [12]. However, many other factors such as different surface forcing or details of the coastal geometry could have affected equatorial sea surface temperatures of this time.

A model run with a land distribution resembling the current configuration of continents, modern surface forcing, and a slightly higher resolution shows a similar behavior in the Atlantic Ocean to that of the ocean in the north-south strip run. The overturning stream function in figure 5-1 shows that water sinks in the North Atlantic near 60°N and rises at the equator, indicating that the modern North Atlantic is in a thermal mode which is very similar to the one calculated for the model with the simple north-south strip of land (figure 4-6). The heat transport per kilometer of zonal ocean extent for the model of the present North Atlantic (figure 5-2) is somewhat similar to the heat transport of the ocean with the north-south strip. The level of heat transport in the model of present is less smooth, possibly as a result of the complicated coastal geometry, and a little larger, probably due to different surface forcing. One might predict that the modern North Atlantic would have a similar mode of heat transport to the ocean with the north-south strip because both oceans face a solid strip of land from the north pole to well below the equator. The pattern of circulation in the southern hemisphere may be different because of the circumpolar passageway. These results support the idea that the topological constraints of the Atlantic play a role in determining its heat transport capacity.

In conclusion, landmass distribution can be very important in determining levels of ocean heat transport. Two very different modes of ocean circulation with very different levels of heat transport can be produced with the same forcings but different configurations of land. If one of the hemispheres is devoid of land, a haline mode

of circulation may be more likely to develop. In this mode ocean heat transport is reduced by a factor of two, and pole-equator temperature gradients are elevated. A significant or complete barrier between the poles tends to produce a thermal mode of circulation with a lower pole-equator temperature gradient. Narrow equatorial passageways around the globe do not appear to produce dramatically different results from solid north-south barriers and may slightly enhance ocean heat transport.

Further research should be done to test the effects of passageways of different sizes and at different latitudes. One of the most exciting results from this work is the discovery of a deep-reaching, stable haline mode for the land configuration similar to that of the late Proterozoic 600 Ma ago. Further study of this mode could determine under what range of surface forcings and land distributions it is stable. Another key step in determining exactly how large an effect topological constraints can have on ocean heat transport is to run simulations with a coupled ocean and atmosphere because the heat transport of one is thought to be closely linked to the transport of the other. Nevertheless, these preliminary results suggest that interpretations of the paleorecord and of the effects of other climate factors should attempt to include an analysis of the mode of ocean circulation and quantity of ocean heat transport suggested by the continental configurations of that period.

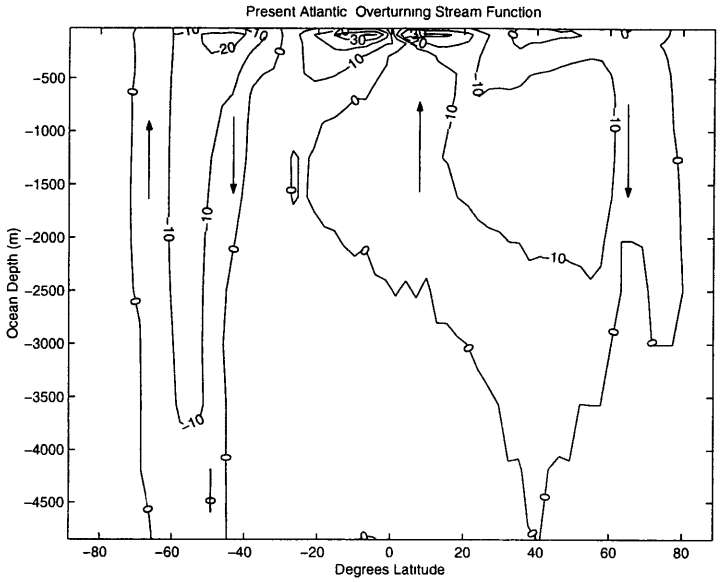

Figure 5-1: **Horizontally integrated vertical stream function for a model of the present-day Atlantic Ocean.** The circulation in the northern hemisphere of the Atlantic is in a thermal mode very similar to the one modeled for the north-south strip of land shown in figure 4-6.

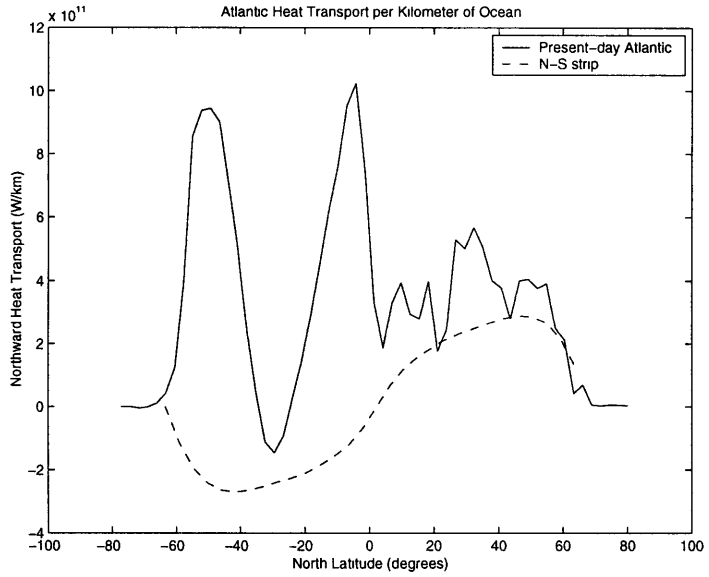

Figure 5-2: **Modern Atlantic heat transport per kilometer of zonal extent.** The modeled heat transport per kilometer of zonal ocean extent for the north Atlantic looks somewhat similar to that calculated for the north-south strip of land. Both oceans are in a thermal mode. The heat transport in the southern hemisphere looks very different, possibly because of the Antarctic circumpolar current.

Bibliography

[1] E. J. Barron, P. J. Fawcett, and W. H. Peterson. A "simulation" of the mid-Cretaceous climate. *Paleoceanography*, 10:953–962, 1995.

[2] E. J. Barron, W. H. Peterson, D. Pollard, and S. Thompson. Past climate and the role of ocean heat transport: Model simulations for the Cretaceous. *Paleoceanography*, 8:785–798, 1993.

[3] B. C. Carissimo, A. H. Oort, and T. H. Vonder Harr. Estimating the meridional energy transports in the atmosphere and ocean. *Journal of Physical Oceanography*, 15:82–91, 1985.

[4] Thomas J. Crowley and Gerald R. North. *Paleoclimatology.* Oxford University Press, New York, 1996.

[5] L. A. Frakes, J. E. Francis, and J. I. Syktus. *Climate Modes of the Phanerozoic.* Cambridge University Press, New York, 1994.

[6] E. Maier-Reimer, U. Mikolajewicz, and T. Crowley. Ocean general circulation model sensitivity experiment with an open central American isthmus. *Paleoceanography*, 5:349–366, 1990.

[7] J. Marshall, C. Hill, L. Perelman, and A. Adcroft. Hydrostatic, quasi-hydrostatic, and non-hydrostatic ocean modeling. *Journal of Geophysical Research*, 102:5733–5752, 1997.

[8] U. Mikolajewicz and T. J. Crowley. Response of a coupled ocean/energy balance model to restricted flow through the central American isthmus. *Paleoceanography*, 12:429–441, 1997.

[9] D. Potter. *Computational Physics.* John Wiley, New York, 1976.

[10] C. J. Poulsen, D. Seidov, E. J. Barron, and W. H. Peterson. The impact of paleogeographic evolution on the surface oceanic circulation and the marine environment within the mid-Cretaceous Tethys. *Paleoceanography*, 13:546–559, 1998.

[11] L. C. Sloan, J. C. G. Walker, and T. C. Moore Jr. Possible role of oceanic heat transport in Early Eocene climate. *Paleoceanography*, 10:347–356, 1995.

[12] S. M. Stanley. New horizons for paleontology, with two examples: the rise and fall of the Cretaceous Supertethys and the cause of the modern ice age. *Journal of Paleontology*, 69:999–1007, 1995.

[13] J. M. Toole. New data on deep sea turbulence shed light on vertical mixing. *Oceanus*, 39(2):33–35, 1996.

[14] Brian F. Windley. *The Evolving Continents.* John Wiley and Sons, New York, 1995.

[15] R. Zhang, M. J. Follows, J. P. Grotzinger, and J. Matshall. Could the Late Permian deep ocean have been anoxic? Submitted to *Paleoceanography*, 1999.

[16] A. M. Ziegler. In W. S. MacKerrow and C. R. Scotese, editors, *Paleozoic Paleogeography and Biogeography*, pages 363–379. Geological Society Memoir, Oxford, 1990.